Projectile electron loss with a molecular hydrogen target

W. E. Meyerhof, H.-P. Hülskötter, and Qiang Dai
Department of Physics, Stanford University, Stanford, California 94305

J. H. McGuire and Y. D. Wang
Department of Physics, Kansas State University, Manhattan, Kansas 66506
(Received 6 December 1990)

We examine the effect of a molecular hydrogen target, as contrasted with an atomic target, on one-electron-projectile electron loss within the framework of the plane-wave Born approximation. Two different approaches are explored: (1) the use of an approximate molecular wave function due to Weinbaum, and (2) the use of a modified form factor for the two atoms in the H_2 molecule. The resulting cross-section expressions are compared with experimental cross sections for electron loss by various one-electron projectiles. We find that for a projectile atomic number larger than 5, molecular effects are negligible in total cross sections and then the electron-loss cross section per molecule is just equal to twice the total cross section per atom.

I. INTRODUCTION

In a recent series of experiments on projectile electron loss by H_2 and He targets, the role of the target-electron–projectile-electron interaction in the projectile-electron ionization process has been explored.[1–3] Although from a theoretical point of view, it would have been simpler to use an atomic H^0 target, it is much easier to use a molecular target. Hence, it is necessary to examine theoretically the influence of the molecular nature of the target on the projectile electron loss cross section, which, so far, has been calculated only for atomic targets, as far as we are aware.[4–9]

The influence of the molecular nature of a target on electron *capture* by a projectile has been considered by Tuan and Gerjuoy[10] and by Wang *et al.*[11] Use is made there of an approximate H_2 wave function proposed by Weinbaum.[12] One finds an interference effect due to the two atomic centers in the molecule[13] and a modification of the transition matrix elements due to the molecular wave function. In projectile electron loss, the situation is similar.

II. THEORY

A. Two-center interference effect

The simplest case to treat is electron loss from a one-electron projectile. Extension to a many-electron projectile is not difficult. It requires summation over the individual electrons, assuming multielectron effects in the projectile are ignored. In the plane-wave Born approximation (PWBA), nuclear screening constants and effective hydrogenic binding energies must be introduced.[14]

Figure 1 shows the coordinate system we use in the following discussion. The projectile with nuclear charge Z_p carries one electron in its $1s$ state. The target is a hydrogen molecule with internuclear separation ρ. Each of the two target nuclei carries one electron. In the center-of-mass system, the Hamiltonian H, expressed in atomic units, is given by

$$H=-\frac{\nabla_p^2}{2M}+\left[-\frac{\nabla^2}{2}-\frac{Z_p}{r}\right]+\left[-\frac{(\nabla')^2}{2}-\frac{1}{r'}-\frac{(\nabla'')^2}{2}-\frac{1}{r''}+\frac{1}{|\mathbf{r}'-\mathbf{r}''|}\right]+V\ , \tag{1}$$

where M is the reduced mass of the projectile. The first term in the Hamiltonian is the kinetic energy of the projectile nucleus, the second term is the kinetic and potential energy of the projectile electron with respect to its nucleus, and the third term is the kinetic and potential energy of the two target electrons. The rotational and vibrational degrees of freedom of the molecule are neglected. The last term V is the perturbation interaction, which is given by

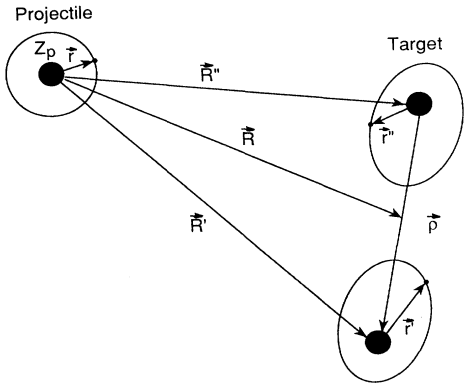

FIG. 1. Coordinate system for one-electron-projectile—H_2-molecule collision.

$$V=\left[\frac{Z_p}{R'}+\frac{Z_p}{R''}\right]+\left[-\frac{Z_p}{|\mathbf{R}'+\mathbf{r}'|}-\frac{Z_p}{|\mathbf{R}''+\mathbf{r}''|}\right]+\left[-\frac{1}{|\mathbf{R}'-\mathbf{r}|}-\frac{1}{|\mathbf{R}''-\mathbf{r}|}\right]+\left[\frac{1}{|\mathbf{R}'+\mathbf{r}'-\mathbf{r}|}+\frac{1}{|\mathbf{R}''+\mathbf{r}''-\mathbf{r}|}\right] . \quad (2)$$

Here, the first term describes the interaction between the projectile nucleus and the target nuclei, the second term the interaction between the projectile nucleus and the target electrons, the third term the interaction between the projectile electron and the target nuclei, and the fourth term the interaction between the projectile electron and the target electrons.

Generally, the cross section can be written

$$\sigma=\frac{M^2}{4\pi^2}\sum_{\text{final states}}\int|f|^2d\Omega=\frac{1}{2\pi v^2}\sum_{\text{final states}}\int q\,dq\,|f(\mathbf{q})|^2 , \quad (3)$$

where M is the reduced mass of the system, $\mathbf{q}$ denotes the momentum transferred in the collision, v is the collision velocity, and in the PWBA, $f(\mathbf{q})$ is the scattering amplitude given by

$$f(\mathbf{q})=-\int d\mathbf{R}\langle\Psi_f|V|\Psi_i\rangle e^{i\mathbf{q}\cdot\mathbf{R}} . \quad (4)$$

Equation (3) assumes aximuthal symmetry about $\mathbf{q}$. In Eq. (4), Ψ_f and Ψ_i denote the initial- and final-state wave functions which, with the neglect of any exchange interaction, are given by

$$\Psi_f=\Phi_N(r',r'')\phi_f(r) \text{ and } \Psi_i=\Phi_0(r',r'')\phi_i(r) , \quad (5)$$

where $\Phi(r',r'')$ and $\phi(r)$ are the internal wave functions of the molecular target and atomic projectile and $N,0$ and f,i refer to the final, initial, target and projectile states, respectively. The sum in Eq. (3) is over all final states relevant to the collision under consideration. Substitution of Eq. (5) into Eq. (4) gives

$$f(\mathbf{q})=-\int\int\int\int d\mathbf{R}\,d\mathbf{r}'d\mathbf{r}''d\mathbf{r}\,\Phi_N^*(r',r'')\phi_f^*(r)\times\left[\left[-\frac{1}{|\mathbf{R}'-\mathbf{r}|}-\frac{1}{|\mathbf{R}''-\mathbf{r}|}\right]+\left[\frac{1}{|\mathbf{R}'+\mathbf{r}'-\mathbf{r}|}+\frac{1}{|\mathbf{R}''+\mathbf{r}''-\mathbf{r}|}\right]\right]e^{i\mathbf{q}\cdot\mathbf{R}}\Phi_0(r',r'')\phi_i(r) \quad (6)$$

$$\equiv f_{\mathrm{EN}}(\mathbf{q})+f_{\mathrm{EE}}(\mathbf{q}) . \quad (7)$$

The first two terms in Eq. (2) do not contribute to the scattering amplitude since they do not involve the projectile-electron coordinate $\mathbf{r}$ and the integrals are zero due to the orthogonality of the projectile wave functions. The two terms in the integrand of f, due to the projectile-electron–target-nuclei and projectile-electron–target-electron interactions, give rise to the amplitudes f_{EN} and f_{EE}, respectively. In Appendix A it is shown that the evaluation of Eq. (6) results in the expression

$$f(q)=\frac{8\pi}{q^2}\cos\left[\frac{\mathbf{q}\cdot\boldsymbol{\rho}}{2}\right]F_p(q)F_t^N(q) , \quad (8)$$

where F_p is the projectile form factor

$$F_p(q)=\int d\mathbf{r}\,\phi_f^*e^{i\mathbf{q}\cdot\mathbf{r}}\phi_i(r) \quad (9)$$

and F_t^N is the form factor for one electron in the target molecule, briefly called the target form factor,

$$F_t^N(q)=\langle\Phi_N|\delta_{N0}-e^{i\mathbf{q}\cdot\mathbf{r}'}|\Phi_0\rangle . \quad (10)$$

In F_t^N, the Dirac δ function term can be traced to f_{EN}, and the other term to f_{EE} (see Appendix A). The two-center interference effect appears in the term $2\cos(\mathbf{q}\cdot\boldsymbol{\rho}/2)$ in Eq. (8). As shown in Appendix A, it arises due to the translation of one center relative to the other, introducing phase factors $\exp(\pm i\mathbf{q}\cdot\boldsymbol{\rho}/2)$ with respect to the molecular center of mass. This interference effect is identical to that for elastic collisions.[13] Substitution of Eq. (8) into Eq. (3) gives the desired cross section for projectile-electron excitation or electron loss by collision with a H_2 molecule.

If in Eq. (3) one separates out those collisions that leave the target in its ground state,[4] one can write for the case of projectile electron loss,

$$\sigma=\sigma_s+\sigma_a , \quad (11)$$

where

$$\sigma_s=\frac{8\pi}{v^2}\int_0^\infty d\varepsilon\int_{q_{\min(s)}}^{q_{\max(s)}}q^{-3}dq\,|F_p(q)|^2\times\int(4\pi)^{-1}d\Omega_\rho|1-F_t(q)|^2\times2[1+\cos(\mathbf{q}\cdot\boldsymbol{\rho})] \quad (12)$$

and

$$\sigma_a=\frac{8\pi}{v^2}\int_0^\infty d\varepsilon\sum_{N\neq0}\int_{q_{\min(a)}}^{q_{\max(a)}}q^{-3}dq\,|F_p(q)|^2\times\int(4\pi)^{-1}d\Omega_\rho|F_t^N(q)|^2\times2[1+\cos(\mathbf{q}\cdot\boldsymbol{\rho})] . \quad (13)$$

Here, F_t without a superscript denotes $F_t^N(N=0)$, and $q_{\min}$ and $q_{\max}$ are the minimum and maximum momentum transfers to the projectile necessary to eject projectile electrons with kinetic energy ε and, in σ_a, to also excite or ionize the target electrons. For heavy projectiles, $q_{\max}$ may be set equal to infinity and $q_{\min}$ can be approximated by[14,15]

$$q_{\min(s)}=(I_p+\varepsilon)/v \ , \tag{14}$$

$$q_{\min(a)}=(I_p+\varepsilon+\Delta E_t^N)/v \ , \tag{15}$$

where I_p is the projectile-electron ionization energy and ΔE_t^N is the target excitation energy. The integrals over the solid angle $d\Omega_\rho$ in Eqs. (12) and (13) generally cannot be immediately performed because the molecular form factor F_t^N is orientation dependent.[11] In Appendix D we show that only small errors are introduced in the cross sections if this form factor is orientation averaged before integrating over $d\Omega_p$.

In the literature, σ_s and σ_a have been called the elastic and inelastic,[4] or screening and antiscreening,[7] cross sections, and σ_a has also been recognized as a two-center electron-electron scattering correlation.[16] We use the nomenclature of Ref. 7.

B. Closure approximation

The main difficulty in evaluating Eq. (11) lies in the summation over excited target states in σ_a [Eq. (13)]. This cannot be executed except for atomic H,[4] because $q_{\min(a)}$ depends on the target excitation energies [Eq. (15)]. Hartley and Walters[9] have suggested that by modeling the actual target states as hydrogenic states, one can bypass this problem, especially if further simplifying assumptions are made. Typically, though, one interchanges the summation over target states and the integration over q in Eq. (13) after replacing ΔE_t^N in Eq. (15) by a suitably chosen average energy. Various proposals have been made, which are discussed in Ref. 9. In the calculations shown below, we have set the average value of ΔE_t^N equal to the ionization energy I_t of H_2, thus replacing $q_{\min(a)}$ by the average momentum transfer

$$\bar{q}_{\min(a)}=(I_p+\varepsilon+I_t)/v \ . \tag{16}$$

Montenegro and Meyerhof have shown that a better value for $\bar{q}_{\min(a)}$ can be obtained directly from the theory by making use of an energy-weighted sum rule for $|F_t^N|^2$ derived by Bethe.[17,18] The value for $\bar{q}_{\min(a)}$ found is practically that for ionization of the projectile by *free* electrons of velocity v. This agrees with the fact that σ_a is purely due to the target-electron–projectile-electron interaction (because of the factor δ_{N0} in f_{EN}) and also justifies a similar assumption for $\bar{q}_{\min(a)}$ made in Ref. 9.

Once the summation over target states has been interchanged with the integration over q in Eq. (13), closure[19] can be used to yield

$$\sigma_a=\frac{8\pi}{v^2}\int_0^\infty d\varepsilon\int_{\bar{q}_{\min(a)}}^\infty q^{-3}dq\,|F_p(q)|^2 \times\int(4\pi)^{-1}d\Omega_\rho[1-|F_t(q)|^2] \times 2[1+\cos(\mathbf{q}\cdot\boldsymbol{\rho})] \ . \tag{17}$$

Unfortunately, the choice of a constant average target excitation energy in $\bar{q}_{\min(a)}$ produces very poor results at low projectile velocities, because it ignores the kinematic requirement that the target electron(s) must have enough energy in the projectile frame to ionize the projectile electron.[8] If the target electrons were free, σ_a would have a sharp threshold at the velocity v given by

$$v^2/2\geq I_p \ . \tag{18}$$

Anholt[8] made the *ad hoc* proposal that σ_a should be modified by multiplying it with the factor $\sigma_e(v)/\sigma_p(v)$, where σ_e is the free-electron and σ_p the free-proton cross section for projectile electron loss at the velocity v. Then

$$\sigma_a^{\mathrm{mod}}=\sigma_a\sigma_e(v)/\sigma_p(v) \ . \tag{19}$$

This prescription agrees well with the calculations of Bates and Griffing[4] for electron loss in H^0+H^0 collisions, both below and above the threshold velocity. But the prescription produces an artificially sharp threshold, whereas in reality the electron momentum distribution in the target smears out the threshold.[4,20] The proposals of Refs. 9 and 17 avoid any such *ad hoc* multiplying factor for σ_a and automatically produce a smooth threshold effect through the appropriate choice of $\bar{q}_{\min(a)}$. Nevertheless, because of ease of programming, we have used Eq. (19) in the calculations shown below. Also, we have shown that the various approximate treatments for σ_a in Refs. 8, 9, and 17 give very similar results as the projectile atomic number increases.

C. Effective squared target charges

For the remaining discussion, it is useful to define effective squared target charges $S_s(q)$ and $S_a(q)$ by the equations

$$\sigma_{s,a}=\frac{8\pi}{v^2}\int_0^\infty d\varepsilon\int_{q_{\min(s,a)}}^\infty q^{-3}dq\,|F_p(q)|^2S_{s,a}(q) \ , \tag{20}$$

$$S_s(q)=\int(4\pi)^{-1}d\Omega_\rho 2[1+\cos(\mathbf{q}\cdot\boldsymbol{\rho})]|1-F_t(q)|^2 \ , \tag{21}$$

$$S_a(q)=\int(4\pi)^{-1}d\Omega_\rho 2[1+\cos(\mathbf{q}\cdot\boldsymbol{\rho})][1-|F_t(q)|^2] \ . \tag{22}$$

The Anholt modification, Eq. (19), still has to be applied to σ_a.

We now proceed to evaluate Eq. (20) in three ways, by using the Weinbaum wave function and by obtaining the molecular form factor F_t through two different modifications of the atomic form factor for H^0.

D. Modified Weinbaum molecular form factor

Weinbaum[12] has proposed a simple wave function for the H_2 ground state which takes into account atomic and

ionic configurations:[21]

$$\Phi_0 = N\{c[\psi(\mathbf{r}')\phi(\mathbf{r}'')+\psi(\mathbf{r}'')\phi(\mathbf{r}')] + \psi(\mathbf{r}')\psi(\mathbf{r}'')+\phi(\mathbf{r}')\phi(\mathbf{r}'')\} \ . \quad (23)$$

The coordinate system of Fig. 1 is used. Each wave function is of the form of a $1s$ hydrogenic wave function,

$$\psi(\mathbf{r}) = Z^{3/2}e^{-Zr}/\pi^{1/2} \ , \quad (24)$$

$$\phi(\mathbf{r}) = \psi(\mathbf{r}-\boldsymbol{\rho}) \ . \quad (25)$$

Here, Z is an effective atomic number, to be chosen later. The normalizing factor N is[12]

$$N = 1/\{2[(1+c^2)(1+\Delta^2)+4c\Delta]\}^{1/2} \ , \quad (26)$$

where Δ is the overlap integral[11]

$$\Delta = \int d\mathbf{r}\,\psi(\mathbf{r})\phi^*(\mathbf{r}) = [1+Z\rho+(Z\rho)^2/3]e^{-Z\rho} \ . \quad (27)$$

By minimizing the binding energy of the H_2 molecule ($\rho = 1.417$ a.u.), Weinbaum[12] obtained the values $c = 3.9$ and $Z = 1.193$, yielding $\Delta = 0.672$ and $N = 0.1212$.

The evaluation of the target form factor

$$F_t(q) = \int d\mathbf{r}'\,d\mathbf{r}''|\Phi_0|^2 e^{i\mathbf{q}\cdot\mathbf{r}'} \quad (28)$$

is straightforward, but tedious. The final result is

$$F_t = a(1+e^{i\boldsymbol{\rho}\cdot\mathbf{q}})F + a'F' \ . \quad (29)$$

Here, F is the H^0 atomic form factor[15]

$$F(q) = \int d\mathbf{r}|\psi(\mathbf{r})|^2 e^{i\mathbf{q}\cdot\mathbf{r}} = 1/[1+(q/2Z)^2]^2 \quad (30)$$

and F' is the displaced form factor

$$F'(q) = \int d\mathbf{r}\,\psi(\mathbf{r})\psi^*(\mathbf{r}-\boldsymbol{\rho})e^{i\mathbf{q}\cdot\mathbf{r}} \ . \quad (31)$$

Also,

$$a = (1+c^2+2c\Delta)N^2 = 0.3153 \ , \quad (32)$$

$$a' = [2\Delta(1+c^2)+4c]N^2 = 0.5496 \ . \quad (33)$$

Analytically, F' can be reduced only to a one-dimensional integral which depends in a complicated manner on the relative orientation of $\boldsymbol{\rho}$ and $\mathbf{q}$.[21] We shown in Appendix B the exact evaluation of F', but we found that the effect of F' on the total cross section is small. Hence, we have also evaluated it crudely for ease in computation. By shifting the origin of coordinates, we approximate the integrand of Eq. (31), namely,

$$\psi(\mathbf{r})\psi^*(\mathbf{r}-\boldsymbol{\rho})e^{i\mathbf{q}\cdot\mathbf{r}} = \psi(\mathbf{r}+\boldsymbol{\rho}/2)\psi^*(\mathbf{r}-\boldsymbol{\rho}/2)e^{i\mathbf{q}\cdot(\mathbf{r}+\boldsymbol{\rho}/2)} \simeq \psi(\mathbf{r})\psi^*(\mathbf{r})e^{i\mathbf{q}\cdot(\mathbf{r}+\boldsymbol{\rho}/2)}\Delta \ .$$

Then, from Eq. (31) it follows that

$$F' \simeq F\Delta e^{i\mathbf{q}\cdot\boldsymbol{\rho}/2} \ , \quad (34)$$

and one obtains

$$F_t \simeq [a(1+e^{i\mathbf{q}\cdot\boldsymbol{\rho}})+be^{i\mathbf{q}\cdot\boldsymbol{\rho}/2}]F \ , \quad (35)$$

where $b = a\Delta = 0.3693$ and F is given by Eq. (30). This is our modified Weinbaum form factor.

Now, the integrals over $d\Omega_\rho$ in Eqs. (21) and (22) can be performed. We denote the effective squared target charges, calculated with the Weinbaum wave function, by $S_s^W(q)$ and $S_a^W(q)$, respectively. Then one finds

$$S_s^W(q) = 2\{1-3aF+(3a^2+b^2)F^2+(6abF^2-3bF)R_1 + [1-4aF+(4a^2+b^2)F^2]R_2 + (2abF^2-bF)R_3+(a^2F^2-aF)R_4\} \ , \quad (36)$$

$$S_a^W(q) = 2\{1-(3a^2+b^2)F^2-6abF^2R_1 + [1-(4a^2+b^2)F^2]R_2 - 2abF^2R_3-a^2F^2R_4\} \ , \quad (37)$$

where

$$R_n = [\sin(nq\rho/2)]/(nq\rho/2), \quad n = 1,2,3,4 \ . \quad (38)$$

Evaluation of Eq. (20) must be done numerically. The results are given below in comparison with results using other expressions for the molecular form factor $F_t(q)$.

E. "Hubbell-Cooper" molecular form factor

Crasemann *et al.*[22] have shown that the photoelectric cross section per H atom in H_2 near 5 and 8 keV is approximately 1.45 times the calculated cross section for a free H^0 atom. Cooper[23] explained this as being due to an increased electronic density at one nucleus in H_2 over that at the H^0 nucleus, which in turn affects the form factor per atom in H_2 at high momentum transfers. Cooper computed the relative increase to be 1.444, in excellent agreement with the experimental enhancement. Incidentally, the Weinbaum wave function predicts a nearly identical enhancement, as shown in Appendix C.

Bentley and Steward[24] computed an orientation-averaged squared H_2 form factor, from which Hubbell *et al.*[25] deduced a form factor per H atom in H_2. In our notation, this can be written

$$\bar{F}_t(q) \simeq \sqrt{2}F_0(q) \ , \quad (39)$$

where $F_0(q)$ is given by Eq. (30) with $Z = 1$. The bar on $\bar{F}_t$ indicates the implied orientation averaging. For $q \gg 1$, this agrees with the enhancement factor found by Cooper.[23] But, for $q \lesssim 0.87$, $\bar{F}_t$ exceeds unity, reaching the value $\sqrt{2}$ at $q = 0$. This would imply a negative effective squared target charge if substituted into Eq. (22). In the calculation shown below we bypass this problem by simply setting $\bar{F}_t = 1$ whenever $\bar{F}_t$ exceeds unity. Theoretically, this is not justifiable. The Weinbaum form factors given in Eqs. (29) or (35) have the correct limiting values $F_t(0) = 1$.

With Eq. (39), the integration over $d\Omega_\rho$ in Eqs. (21) and (22) can be immediately performed, yielding for the "Hubbell-Cooper" effective squared target charges

$$S_s^H = 2(1-\sqrt{2}F_0)^2(1+R_2) , \quad (40)$$

$$S_a^H = 2(1-2F_0^2)(1+R_2) , \quad (41)$$

considerably simpler than Eqs. (36) and (37). Here, R_2 is defined in Eq. (38). Results using these relations are presented in Sec. III. In these calculations, we have used the Cooper factor 1.444, rather than $\sqrt{2}$, in Eq. (39).

F. "Stewart" molecular form factor

The behavior of Eq. (39) at low q values stimulated us to search for a more satisfactory target form-factor expression. Hubbell *et al.*[26] list an orientation-averaged incoherent scattering function $\bar{S}_{\rm inc}$ per H atom in H_2, calculated by Stewart.[27] By using the relation

$$\bar{F}_t = (1-\bar{S}_{\rm inc})^{1/2} , \quad (42)$$

based on Eq. (31) of Ref. 25, we have computed the proportionality factor $g(q)$ in the expression

$$\bar{F}_t(q) = g(q)F_0(q) , \quad (43)$$

where $F_0(q)$ is again the atomic form factor for a free H^0 atom, given in Eq. (30) with $Z=1$. Figure 2 shows the factor $g(q)$. At low q, it has the value unity assuring that $\bar{F}_t(0)=1$, and at high q it appears to oscillate toward the Hubbell-Cooper value 1.444, discussed in Sec. II E. Hence, we believe that Eq. (43) represents a theoretically acceptable improvement over Eq. (39). By trial and error, we have found that the relation

$$g(q) \simeq 1+k_1/[1+(k_2/q^2)\cos(k_3 q)] , \quad (44)$$

with $k_1=0.444$, $k_2=3.8$, $k_3=0.673$, gives a fit within 2% up to $q=3.5$ to Eq. (42). Above $q=3.5$, $F_0(q)$ lies below 0.1, so that the small deviation shown in Fig. 2 is of no importance in the final cross section.

Using Eq. (43), one finds from Eqs. (21) and (22) the Stewart effective squared target charges

$$S_s^S = 2(1-gF_0)^2(1+R_2) , \quad (45)$$

$$S_a^S = 2[1-(gF_0)^2](1+R_2) , \quad (46)$$

where R_2 is defined in Eq. (38).

The Hubbell-Cooper and Stewart models both make use of a form factor $\bar{F}_t$ which really is the square root of an orientation-averaged squared form factor $\langle |F_t|^2 \rangle$ [see Eqs. (32) and (31), respectively, in Ref. 25]. In Appendix D we discuss what error may be introduced by this procedure. We find that, had we used an orientation-averaged "Weinbaum" squared form factor, the electron-loss cross section would be lowered by less than $\sim 15\%$ for $Z_p=1$, by less than $\sim 7\%$ for $Z_p=2$, and progressively less for higher values of Z_p, in the region of validity of the PWBA.

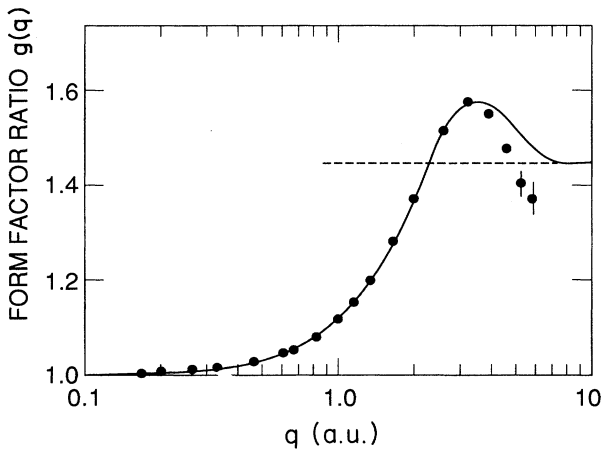

FIG. 2. Proportionality factor $g(q)$ between molecular and atomic hydrogen form factors calculated using tabulation in Ref. 26. The curve gives the fit represented by Eq. (44). The dashed horizontal line is the Hubbell-Cooper value 1.444.

III. RESULTS AND COMPARISON WITH EXPERIMENT

Using the models presented in Sec. II D to Sec. II F, we have computed the electron-loss cross section [Eq. (11)] for one-electron projectiles scattered by H_2. For the Weinbaum, Hubbell-Cooper, and Stewart models, respectively, we denote the cross sections by $\sigma^{\rm W}$, $\sigma^{\rm H}$, and $\sigma^{\rm S}$. We have searched the literature in order to confront the theory with two types of experimental data: (1) the ratio

$$r_{21} = \sigma(H_2)/\sigma(H^0) \quad (47)$$

for electron loss in molecular and atomic hydrogen and (2) the absolute cross section $\sigma(H_2)$. We thought that the ratio r_{21} is particularly significant since it might cancel out possible defects in the PWBA theory as well as some systematic experimental errors. Unfortunately, we have found measurements of r_{21} only for the one-electron projectiles H^0 and Li^{2+}.

For the calculation of $\sigma(H^0)$ we have used Eq. (12) for σ_s and the closure expression analogous to Eq. (17) for σ_a, with $F_t(q)$ replaced by $F_0(q)$ and $2(1+\cos\boldsymbol{\rho}\cdot\mathbf{q})$ replaced by unity. Also, we have applied the Anholt modification, Eq. (19). This keeps the theoretical treatment near the electron-electron threshold [Eq. (18)] consistent between $\sigma(H_2)$ and $\sigma(H^0)$. In principle, a better calculation is available for $\sigma(H^0)$ by using the Bates-Griffing expressions.[4]

A. Effective squared target charge

The three models we have computed differ only in the effective squared target charges S_s and S_a. These are shown in Figs. 3(a) and 3(b). The wavy nature of the curves is due to the interference effect. At high q, the three models converge. At low q, they differ appreciably, with the highest suppression (largest F_t) occurring for the Hubbell-Cooper model. We now examine which region of q is relevant.

The integrations over q in the cross sections σ_s and σ_a, Eqs. (21) and (22), have the lower limits $q_{\min(a)}$, Eq. (14), and $\bar{q}_{\min(a)}$, Eq. (16). The lowest values for these limits,

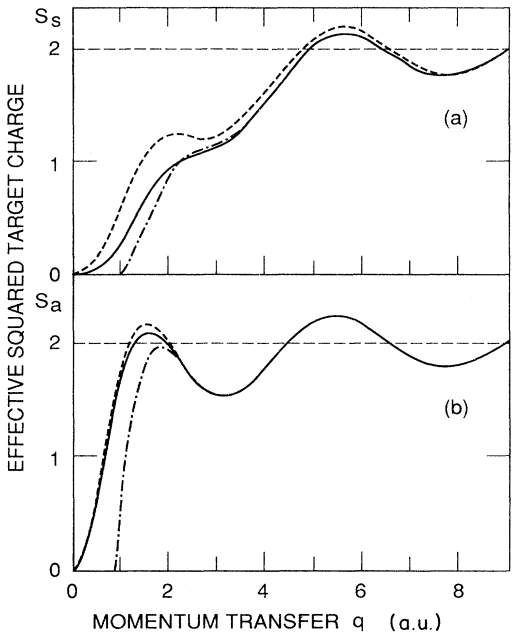

FIG. 3. Effective squared target charges: (a) for screening and (b) for antiscreening part of electron-loss cross section. The short-dashed, solid, and dash-dotted curves represent the Weinbaum, Stewart, and Hubbell-Cooper models, respectively. The latter is cut off below $q=0.87$ for reasons discussed in Sec. II E.

$q^0_{\min(s)}$ and $\bar{q}^0_{\min(a)}$, occur for zero electron energy in the c.m. frame, $\varepsilon=0$, and are given by

$$q^0_{\min(s)}=I_p/v,\quad \bar{q}^0_{\min(a)}=(I_p+I_t)/v\ , \tag{48}$$

where I_p and I_t are the projectile and target ionization energies, respectively. Let us assume a typical projectile velocity to be the electron-electron threshold velocity given in Eq. (18), $v_{\rm th}=(2I_p)^{1/2}$. Then, with $I_p=Z_p^2/2$ and $I_t=Z_t^2/2$, one finds

$$q^0_{\min(s)}=Z_p/2,\quad \bar{q}^0_{\min(a)}=(Z_p^2+1)/2Z_p\ . \tag{49}$$

(Actually, for H_2, $Z_t^2=1.15$.) Since below we discuss results for $Z_p=1$ to 8, from Fig. 3 we expect quite different cross sections for the three models at low Z_p, but similar results at high Z_p, especially since the $1/q^3$ factor in the cross-section expressions emphasizes the lowest q region above $q_{\min}$ of $S(q)$.

B. Region of validity of the PWBA

Before confronting the cross-section models with experimental data, it is useful to have some idea in which bombarding-energy region the PWBA is expected to be valid. Briggs and Taulbjerg have discussed this topic in detail.[28] The most restrictive condition is

$$Z_pZ_t/v\ll 1\ . \tag{50}$$

It is convenient to express the projectile velocity v in units of the electron-electron threshold velocity (which is just the projectile K-shell Bohr velocity)

$$v=\eta^{1/2}v_{\rm th}=\eta^{1/2}Z_p\ , \tag{51}$$

where η is the ratio of the actual projectile kinetic energy to that at the electron-electron threshold. Then the criterion (50) reduces to

$$\eta\gg Z_t^2\ . \tag{52}$$

Hence, for the H^0+H^0 electron-loss cross section, the PWBA should break down below some bombarding energy considerably higher than 0.025 MeV/u. This agrees with the finding of McClure[29] that the Bates-Griffing calculation[4] deviates from the data below $\sim$0.1 MeV/u.

Briggs and Taulbjert reasoned that for total cross sections the validity criterion for the PWBA is not as strict as for differential cross sections. They find that, if $Z_p\gg Z_t$, the condition (52) is relaxed approximately to

$$\eta\gg Z_t^2/200\ . \tag{53}$$

For $O^{7+}+H_2$ electron loss, for example, the PWBA should then be valid down to bombarding energies lying far below the electron-electron threshold.

C. Loss cross-section ratio for H_2 and H^0 targets

Figures 4 and 5 present our model calculations and the corresponding data[29–31] for the cross-section ratio r_{21} [Eq. (47)] for $Z_p=1$ and 3. As noted in Sec. III B, for $Z_p=1$ one would expect the PWBA to break down far above $\eta=1$ and this is borne out. The energy corresponding to $\eta=1$ is marked by an arrow in Fig. 4 and in all subsequent figures. Qualitatively, the dip in r_{21} at low energies is reproduced by the theory, but this may be fortuitous. The very low value of r_{21} for the Hubbell-Cooper model is caused by our artificial cutoff of the integral over q in $\sigma(H_2)$ whenever $\bar{F}_t>1$, discussed in Sec. II E. This suppresses the important low-q contribution to $\sigma(H_2)$. At energies above 0.1 MeV/u, experiment indicates that r_{21} lies somewhat below 2 in agreement with the Stewart model, but measurements at larger bombarding energies would be desirable.

For $Z_p=3$, the Stewart and Hubbell-Cooper models give similar results (Fig. 5). The Hubbell-Cooper result is not particularly low compared to the others, because now $q^0_{\min}$ is larger than 1.5 [see Eq. (49)] which assures that the artificial cutoff for $\bar{F}_t>1$ does not come into play. The experimental data[31] for r_{21} rise to a value of 2 whereas two models indicate lower values. We note though that for a whole range of many-electron projectiles (C^+, C^{2+}, C^{3+}, B^+, B^{2+}),[32] the experimental data rise slowly toward 2, but stay below this value at the highest bombarding energies measured ($\sim$0.2 MeV/u). Since one would expect the PWBA validity criterion to lie between Eqs. (52) and (53), the large deviation between theory and experiment at lower energies is not unexpected.

For completeness, and to stimulate measurements, we show in Fig. 6 the calculated values of r_{21} for He^+ projectiles. We have also computed r_{21} for C^{5+} and O^{7+}

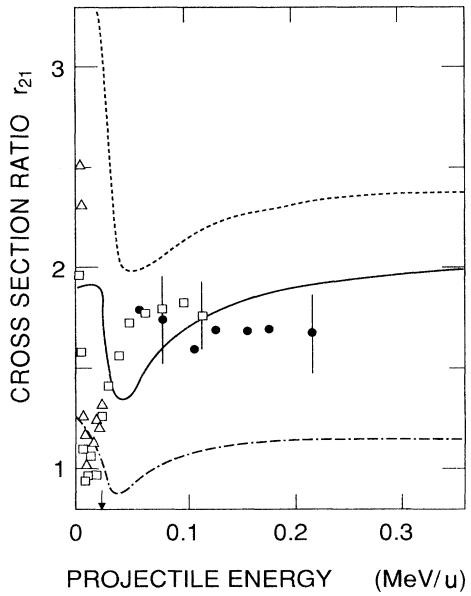

FIG. 4. Ratio r_{21} of H^0 projectile electron-loss cross sections for H_2 and H^0 targets. The short-dashed, solid, and dashed-dotted curves represent the Weinbaum, Stewart, and Hubbell-Cooper model results, respectively. The arrow on the abscissa gives the electron-electron threshold energy ($\eta=1$). The squares give data from Ref. 29, the circles and triangles from Ref. 30. For clarity, some data points have been omitted. To be consistent with the theory, the lower-energy data have been corrected for capture.

projectiles. All the models give the value 2, within 10% for C^{5+} and within 2% for O^{7+}.

D. Loss cross sections for H_2 targets

Figures 7–11 show comparisons of the three models with available data for $\sigma(H_2)$. For clarity of presentation, in some cases we show only some of the available data.

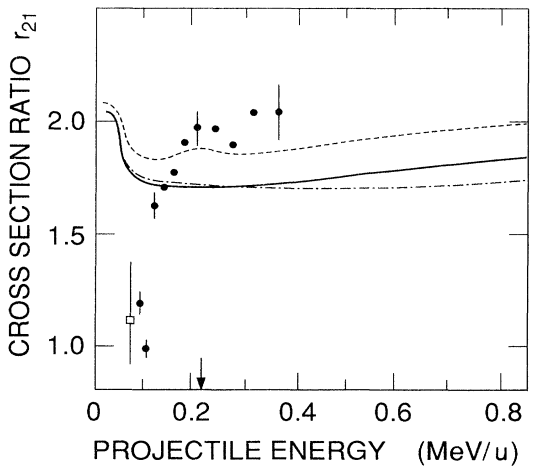

FIG. 5. Same as Fig. 4, but for Li^{2+} projectiles. The data points are from Ref. 31; only the recent, more accurate, data are shown except for the lowest-energy point (square).

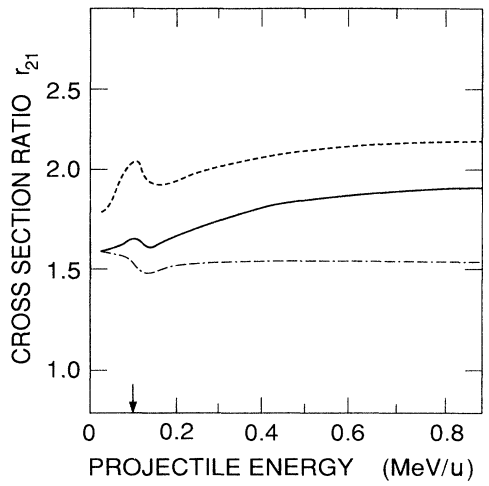

FIG. 6. Same as Fig. 4, but for He^+ projectiles. No data are available.

In Fig. 7 we see the suppression occurring in the Hubbell-Cooper model for $Z_p=1$, discussed in Sec. III C. The other two models lie above the data.[33,34] We already noted above that the PWBA loses its validity below 0.1 MeV/u, i.e., $\eta\approx4$, in accord with criterion (52), applicable here.

For $Z_p=2$ (Fig. 8), the models lie closer to the data[35–37] than for $Z_p=1$, although at the higher energies wide variations are found in the measurements (see Ref. 37). Here, discrepancies between theory and experiment are seen below $\eta\approx2$, as the validity criterion moves to-

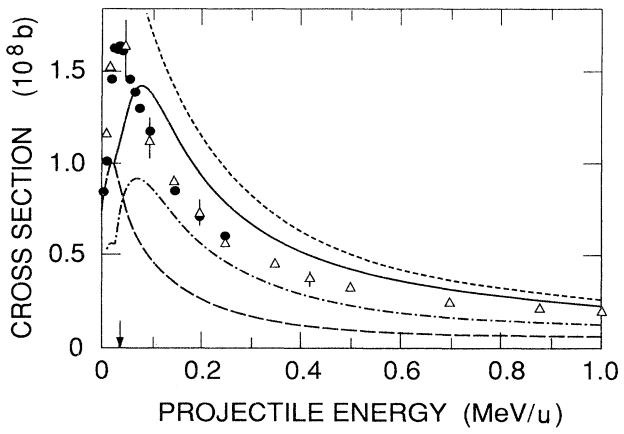

FIG. 7. Electron-loss cross section in H_2 target for H^0 projectiles. The short-dashed, solid, and dash-dotted curves are the Weinbaum, Stewart, and Hubbell-Cooper model results, respectively. The long-dashed curve is the screening cross section σ_s for the Stewart model. The triangles give data from Ref. 34, the circles from Ref. 33. The arrow on the abscissa gives the electron-electron threshold energy ($\eta=1$).

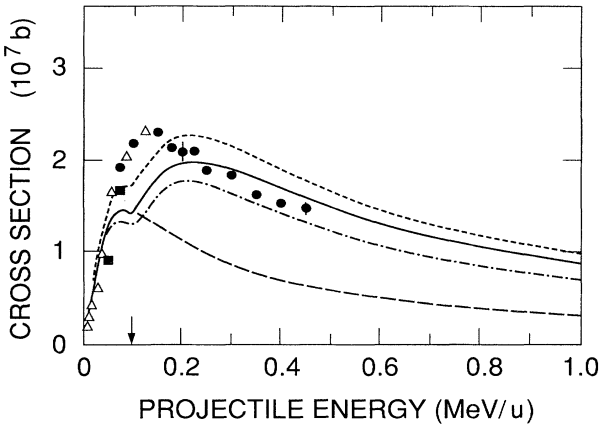

FIG. 8. Same as Fig. 7, but for He^+ projectiles. The solid circles are from Ref. 37, the squares from Ref. 35, and the triangles from Ref. 36.

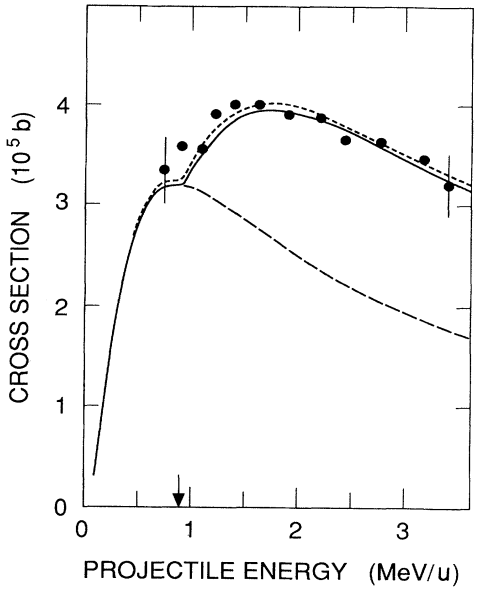

FIG. 10. Same as Fig. 7, but for C^{5+} projectiles. The Hubbell-Cooper model results differ insignificantly from the Stewart model results and are omitted. Data are from Refs. 1–3.

ward Eq. (53).

For $Z_p=3$ (Fig. 9), the Hubbell-Cooper model fits well with the higher energy data.[2,3] A breakdown of the PWBA near $\eta\approx 1$ agrees with the trend of the validity criterion towards lower values of η as Z_p increases. Therefore, the deviations from the lower energy data[31] are expected. For $Z_p=1$ to 3, the results for twice the Bates-Griffing calculation for a H^0 target (now shown) lie very close to the Stewart model, but do not show the artificially sharp electron-electron thresholds introduced by the Anholt modification of σ_a [Eq. (19)].

For $Z_p=6$ and 8, all three models give similar results, as is expected on the basis of the similarity in $S(q)$ at higher q values (Fig. 3). The PWBA validity criterion should approach Eq. (53), but there is no data for one-electron projectiles to check this limit. We note, though, the theory fits the data[1–3] well below the electron-electron threshold for $Z_p=8$, quite in contrast to the situation for $Z_p=1$ or 2. Also, for $Z_p=8$, the results for twice the Bates-Griffing cross section[4] for H^0, shown by triangles in Fig. 11, lie very close to the three models, except right near the electron-electron threshold. This indicates that for $Z_p \gtrsim 6$, there is no need to make any special molecular model calculations. The effective q values are high enough so that the H^0 form factor F [Eq. (30)] and, in turn, the molecular form factor F_t which is propor-

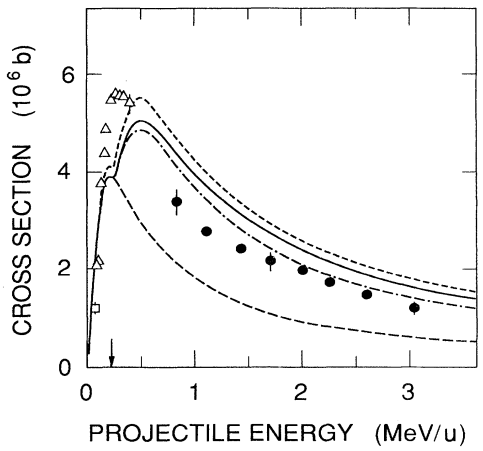

FIG. 9. Same as Fig. 7, but for Li^{2+} projectiles. The solid circles are from Refs. 2 and 3, the triangles from Ref. 31. For the latter, only the most recent, more accurate data are shown, except for the lowest-energy data point (square).

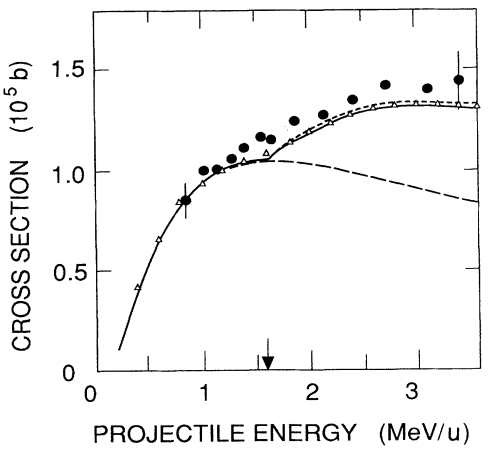

FIG. 11. Same as Fig. 7, but for O^{7+} projectiles. The Hubbell-Cooper model results differ insignificantly from the Stewart model results and are omitted. The triangles give twice the Bates-Griffing results (Ref. 4). Data are from Refs. 1–3.

tional to F are very small. The speculation of Anholt *et al.*[38] that at high-q values the H momentum wave function in H_2 is unaffected by molecular effects, cannot be correct in view of the Cooper enhancement factor.[23]

IV. DISCUSSION AND CONCLUSIONS

The three models we have investigated enhance the ground-state molecular form factor in H_2 at high momentum transfers q and hence, in principle, would be expected to lower the effective target charge $S(q)$ and the electron-loss cross section, compared to twice their value for free H^0 atoms. A lowering of the cross-section ratio is found experimentally at least for H^0 projectiles in the region of validity of the PWBA. Unfortunately, for low-Z projectiles ($Z_p \lesssim 4$), the low-q behavior of the ground-state molecular form factor $F_t(q)$ is much more important than the high-q behavior. Here, the different models give quite different results. At low q, the Hubbell-Cooper model tends to make $F_t(q)$ like that of an atom with $\sqrt{2}$ electrons,[24,25] whereas the Weinbaum model makes F_t look like that of an atom with one electron. The Stewart model lies in between, but at $q=0$ also gives the hydrogenic value. As a consequence of the interference effect in H_2, discussed in Sec. II A, the value of $S(q)$ can lie even above twice the H^0 atomic value in the critical q region just above $q_{\min}$, giving a cross-section ratio of r_{21} greater than 2.

The model calculations provide mixed answers for the absolute molecular target cross sections in the Z_p region below 4, in which molecular effects should make themselves felt. Overall, the Hubbell-Cooper model lies closest to the experimental data points, but for $Z_p=1$ our artificial suppression of q values for $F_t>1$ decreases the cross sections too much. For $Z_p=2$, this model falls somewhat below and for $Z_p=3$ somewhat above the data. For $Z_p=6$ and 8, the data cannot decide between the models.

We conclude that our calculations have met with some success and show that molecular effects should be taken into account in the electron-loss cross sections for one-electron projectiles with $Z_p \lesssim 4$. Experimental data for r_{21} and $\sigma(H_2)$ with H^0, He^+, and Li^{2+} projectiles at higher bombarding energies would be helpful in guiding future theoretical developments in this area.

ACKNOWLEDGMENTS

This work was supported in part by the National Science Foundation Grant No. PHY-86-14650 (Stanford University) and by the Office of Basic Energy Sciences, U.S. Department of Energy (Kansas State University). We thank Dr. M. B. Shah for communicating his results on recent Li^+ and $Li^{2+}+H_2$ electron-loss measurements prior to publication (see Ref. 31).

APPENDIX A: TWO-CENTER INTERFERENCE EFFECT

In Eq. (7), we first consider $f_{\rm EN}(q)$. Making use of the "Bethe integral"[16]

$$\int d\mathbf{R}\frac{e^{i\mathbf{q}\cdot\mathbf{R}}}{|\mathbf{R}-\mathbf{r}|}=\frac{4\pi}{q^2}e^{i\mathbf{q}\cdot\mathbf{r}} \tag{A1}$$

and substituting

$$\mathbf{R}=\mathbf{R}'+\rho/2=\mathbf{R}''-\rho/2\ ,$$

one finds

$$f_{\rm EN}(q)=\frac{4\pi}{q^2}\left[e^{i\mathbf{q}\cdot(\rho/2)}\int\int d\mathbf{R}'d\tau\,\Phi_N^*\phi_f^*\frac{e^{i\mathbf{q}\cdot\mathbf{R}'}}{|\mathbf{R}'+\mathbf{r}|}\Phi_0\phi_i+e^{-i\mathbf{q}\cdot(\rho/2)}\int\int d\mathbf{R}''d\tau\,\Phi_N^*\phi_f^*\frac{e^{i\mathbf{q}\cdot\mathbf{R}''}}{|\mathbf{R}''+\mathbf{r}|}\Phi_0\phi_i\right]$$

$$=\frac{4\pi}{q^2}\left[e^{i\mathbf{q}\cdot(\rho/2)}\int d\tau\,\Phi_N^*\phi_f^*e^{i\mathbf{q}\cdot\mathbf{r}}\Phi_0\phi_i+e^{-i\mathbf{q}\cdot(\rho/2)}\int d\tau\,\Phi_N^*\phi_f^*e^{i\mathbf{q}\cdot\mathbf{r}}\Phi_0\phi_i\right], \tag{A2}$$

where we have abbreviated the integrals over the three electron position vectors by $d\tau$. Equation (A2) can be further simplified by making use of the orthogonality of the target wave function. The final result for the electron-nucleus scattering amplitude is

$$f_{\rm EN}(q)=\frac{8\pi}{q^2}\delta_{N0}\cos\left[\frac{\mathbf{q}\cdot\rho}{2}\right]F_p(q)\ , \tag{A3}$$

where δ is the Dirac δ function and $F_p(q)$ is the projectile form factor defined in Eq. (9). As ρ approaches zero, the scattering amplitude reduces to the result for a target atom with twice the nuclear charge.

Similarly, one finds for the electron-electron scattering amplitude

$$f_{\rm EE}(q)=\frac{4\pi}{q^2}\left[-e^{i\mathbf{q}\cdot(\rho/2)}\int\int d\mathbf{R}'d\tau\,\Phi_N^*\phi_f^*\frac{e^{i\mathbf{q}\cdot\mathbf{R}'}}{|\mathbf{R}'+\mathbf{r}'-\mathbf{r}|}\Phi_0\phi_i-e^{-i\mathbf{q}\cdot(\rho/2)}\int\int d\mathbf{R}''d\tau\,\Phi_N^*\phi_f^*\frac{e^{i\mathbf{q}\cdot\mathbf{R}''}}{|\mathbf{R}''+\mathbf{r}''-\mathbf{r}|}\Phi_0\phi_i\right]$$

$$=\frac{4\pi}{q^2}\left[-F_p(q)e^{i\mathbf{q}\cdot(\rho/2)}\int\int d\mathbf{r}'d\mathbf{r}''\Phi_N^*e^{i\mathbf{q}\cdot\mathbf{r}'}\Phi_0-F_p(q)e^{-i\mathbf{q}\cdot(\rho/2)}\int d\mathbf{r}'d\mathbf{r}''\Phi_N^*e^{i\mathbf{q}\cdot\mathbf{r}''}\Phi_0\right]. \tag{A4}$$

By symmetry, the two spatial integrals in Eq. (A4) are identical so that the two terms can be combined. Adding the two scattering amplitudes f_{EN} and f_{EE} gives Eq. (8).

APPENDIX B: EXACT WEINBAUM FORM FACTOR AND EFFECTIVE SQUARED TARGET CHARGES

Using Cheshire's Fourier transform technique,[21] the displaced form factor in Eq. (31) can be reduced to a one-dimensional integral and the Weinbaum form factor can be expressed as

$$F_t=(1+e^{i\mathbf{q}\cdot\boldsymbol{\rho}})A+\int_0^1 dx\, e^{i(1-x)\mathbf{q}\cdot\boldsymbol{\rho}}B(x)\ , \tag{B1}$$

where $A=aF$ and

$$B(x)=a'2Z^5x(1-x)(3/n^5+3\rho/n^4+\rho^2/n^3)e^{-n\rho}\ ,$$

with

$$n^2=Z^2+x(1-x)q^2\ .$$

By substituting the above "exact" Weinbaum form factor into Eqs. (21) and (22), we can obtain the effective squared target charges numerically and make comparison with the approximate analytical expressions in Eqs. (36) and (37). Defining the following auxiliary functions:

$$W_0=j_0(q\rho)\ ,$$
$$W_1=j_0(2q\rho)\ ,$$
$$W_2=j_0(q\rho(1-x))\ ,$$
$$W_3=j_0(q\rho(2-x))\ ,$$
$$W_4=j_0(q\rho x)\ ,$$
$$W_5=j_0(q\rho(x-y))\ ,$$
$$W_6=j_0(q\rho(1+x-y))\ ,$$
$$W_7=j_0(q\rho(1-x+y))\ ,$$
$$W_8=j_0(q\rho(1+x))$$

and

$$S_1=2(1+W_0)\ ,$$
$$S_2=2A(3+4W_0+W_1)+2\int_0^1 dx\, B(x)(2W_2+W_3+W_4),$$
$$S_3=A^2(6+8W_0+2W_1)+\int_0^1 dx\int_0^1 dy\, B(x)B(y)\times(2W_5+W_6+W_7)$$
$$+2A\int_0^1 dx\, B(x)(7W_2+2W_3+6W_4+W_8)\ ,$$

the effective charges can then be written as

$$S_s^W(q)=S_1-S_2+S_3\ , \tag{B2}$$
$$S_a^W(q)=S_1-S_3\ . \tag{B3}$$

In Fig. 12 we compare numerical results obtained by Eqs. (B2) and (B3) (solid lines) with Eqs. (36) and (37) (dotted lines). Except near $q=2$, the error due to the use of the approximate form factor is much less than 5% for both screening and antiscreening cases. Near $q=2$, the error is less than 10%. The effect on the total cross section for $Z_p=1$ is less than 5% and even less for higher values of Z_p.

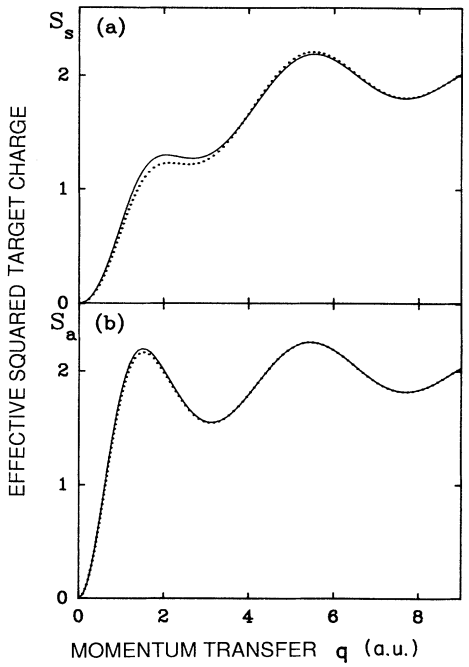

FIG. 12. Comparison of exact and approximate effective squared target charges: (a) for screening and (b) for antiscreening. Solid lines, exact calculation given in Appendix B; dotted lines, approximate calculation by Eqs. (36) and (37).

APPENDIX C: ELECTRON DENSITY AT ONE NUCLEUS IN H_2 IN WEINBAUM MODEL

In terms of the Weinbaum wave function[12] given in Eq. (23), we wish to compute the density $\delta(H_2)$ at one nucleus in the H_2 molecule, say, the lower one in Fig. 1. This is the probability that one electron, say, the lower one, is at this nucleus and the other one anywhere else:

$$\delta(H_2)=2\int d\mathbf{r}''|\Phi_0(\mathbf{r}=0)|^2\ . \tag{C1}$$

The reason for the factor 2 is that the other electron in H_2 can also be at the lower nucleus, and its partner anywhere else. Making use of Eqs. (24) and (25), we find

$$|\Phi_0(\mathbf{r}'=0)|^2=(N^2Z^3/\pi)|G\phi(r'')+H\psi(r'')|^2\ , \tag{C2}$$

where N is given by Eq. (26) and

$$G=c+e^{-Z\rho},\quad H=1+ce^{-Z\rho}\ . \tag{C3}$$

Using the definition of the overlap integral Δ in Eq. (27), one now finds

$$\delta(H_2)=(2N^2Z^3/\pi)(G^2+H^2+2GH\Delta)\ . \tag{C4}$$

From Eq. (24) one sees that with our normalization the density at the nucleus of a free H^0 atom is given by

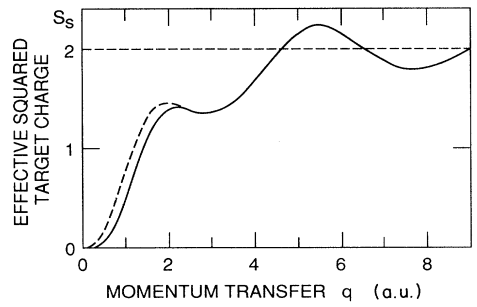

FIG. 13. Squared target charge for screening. The short-dashed curve is for the Weinbaum model, without separate orientation averaging of the squared form factor, as in Fig. 3(a). The solid curve is for the separate orientation averaging described in Appendix D. For S_a, separate orientation averaging produces a change of 1% or less.

$$\delta(H^0)=1/\pi \ , \tag{C5}$$

so that the density ratio $\delta(H_2)/\delta(H^0)$ is immediately obtained from Eq. (C4). With the values for δ, c, Z, Δ, and N given in Sec. II D, one finds $N^2=0.0146$, $G=4.085$, $H=1.720$, giving $\delta(H_2)/\delta(H^0)=1.45$.

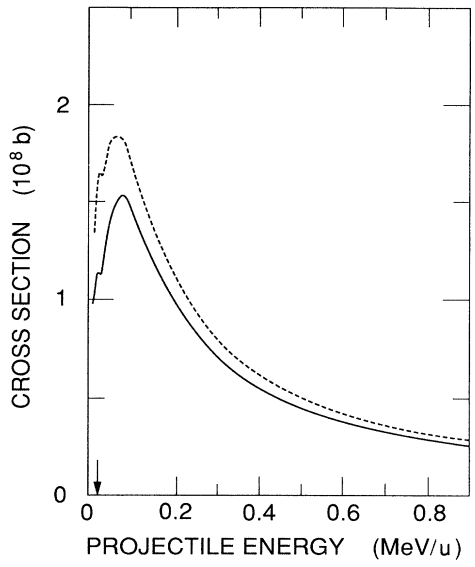

FIG. 14. Electron-loss cross section for H^0 projectiles in H_2 target, according to the Weinbaum model. The short-dashed curve is without separate orientation averaging of the squared form factor, as in Fig. 7. The solid curve is for the separate orientation averaging described in Appendix D.

APPENDIX D: USE OF ORIENTATION AVERAGED FORM FACTOR

In the integrands of Eqs. (21) and (22), the interference terms and the form-factor terms can both depend on the angle between $\mathbf{q}$ and $\boldsymbol{\rho}$, as can be seen from the phase factors in Eqs. (29) or (35) in the Weinbaum model. Hence, one would expect different values for the effective charges and total cross sections, depending on whether the interference and form-factor terms are separately averaged over $d\Omega_\rho$ or not. One would expect that this dependence is strongest if $q_{\min} \lesssim 1/\rho \approx 0.7$ a.u., and progressively weakens as $q_{\min}$ exceeds this value. In view of Eq. (49), this means that separate orientation averaging may be important for $Z_p=1$, but then should become less and less important as Z_p increases.

We noted at the end of Sec. II F that the Hubbell-Cooper and Stewart models actually use orientation-averaged squared form factors, so that the interference term could be orientation averaged separately. We now apply the Weinbaum model to check what errors may be introduced by this (incorrect) procedure in the effective squared target charges and in the total cross section. Using Eq. (35), the orientation-averaged squared form factor is given by the relation

$$\langle |F_t|^2 \rangle / F^2 = \int_{-1}^{1} (dy/2) |a(1+e^{iq\rho y})+be^{iq\rho y/2}|^2 \ , \tag{D1}$$

where $y=\cos\theta_\rho$, θ_ρ being the angle between $\boldsymbol{\rho}$ and $\mathbf{q}$. The evaluation of the integral yields

$$2a^2(1+R_2)+b^2+4abR_1 \ , \tag{D2}$$

where R_n is defined in Eq. (38). The square root of this expression can now be substituted for $g(q)$ in Eq. (43) and one then finds orientation-averaged squared target charges analogous to Eqs. (45) and (46).

In Fig. 13 we compare the Weinbaum model values of $S_s(q)$ and $S_a(q)$ using the orientation-averaged factor $\bar{F}_t=(\langle |F_t|^2 \rangle)^{1/2}$ and using the correct unaveraged factor of Eq. (35). As expected, the effect of orientation averaging appears only at low-q values. For S_a, the difference is less than 1% over the entire range of q.

In Fig. 14 we show the effect of orientation averaging on the electron-loss cross section for H^0 projectiles. We see that orientation averaging results in a lowering of the cross section by less than 15% in the relevant energy region. (We recall that here $\eta \approx 4$ is approximately the lower limit for the validity of the PWBA.) A similar calculation for $Z_p=2$ shows that orientation averaging lowers the cross section by less than 7%, and progressively less for higher values of Z_p. For differential cross sections the situation is completely different. Here one finds a strong orientation dependence, e.g., up to 40% for 1-MeV/u $Li^{2+}+H_2$.[39]

[1]H.-P. Hülskötter, W. E. Meyerhof, E. Dillard, and N. Guardala, Phys. Rev. Lett. **63**, 1938 (1989).

[2]H.-P. Hülskötter, B. Feinberg, W. E. Meyerhof, A. Belkacem, J. R. Alonso, L. Blumenfeld, E. D. Dillard, H. Gould, N. Guardala, G. F. Krebs, M. A. McMahan, M. E. Rhoades-Brown, B. S. Rude, J. Schweppe, D. W. Spooner, K. Street, P. Thieberger, and H. E. Wegner, Phys. Rev. A (to be published).

[3]H.-P. Hülskötter, Ph.D. thesis, Stanford University, 1990.

[4]D. R. Bates and G. Griffing, Proc. Phys. Soc. London, Sect. A **66**, 961 (1953); **67**, 663 (1954); **68**, 90 (1955).

[5]K. L. Bell, V. Dose, and A. E. Kingston, J. Phys. B **2**, 831 (1969).

[6]K. L. Bell and A. E. Kingston, J. Phys. B **4**, 162 (1971).

[7]J. H. McGuire, N. Stolterfoht, and P. R. Simony, Phys. Rev. A **24**, 97 (1981).

[8]R. Anholt, Phys. Lett. **144A**, 126 (1986).

[9]H. M. Hartley and H. R. J. Walters, J. Phys. B **20**, 1983 (1987).

[10]T. F. Tuan and E. Gerjuoy, Phys. Rev. **117**, 756 (1960).

[11]N. C. Deb, A. Jain, and J. H. McGuire, Phys. Rev. A **38**, 3769 (1988); Y. D. Wang, J. H. McGuire, and R. D. Rivarola, *ibid.* **40**, 3673 (1989).

[12]S. Weinbaum, J. Chem. Phys. **1**, 593 (1933). Our definition of ρ is equal to Weinbaum's ρ divided by Z. We follow the original definition of c, and not that in Ref. 11.

[13]N. F. Mott and H. S. W. Massey, *The Theory of Atomic Collisions* (Oxford University Press, London, 1965), Sec. 3.1.

[14]E. Merzbacher and H. W. Lewis, *Handbuch der Physik* (Springer, Berlin, 1958), Vol. 34, p. 166.

[15]H. A. Bethe, Ann. Phys. (Leipzig) **5**, 325 (1930).

[16]N. Stolterfoht, Phys. Scr. **42**, 192 (1990).

[17]E. C. Montenegro and W. E. Meyerhof, Phys. Rev. A **43**, 2289 (1991).

[18]H. A. Bethe and R. Jackiw, *Intermediate Quantum Mechanics* (Benjamin, New York, 1968), Eqs. (17)–(34).

[19]N. F. Mott and H. S. W. Massey, Ref. 13, Sec. 7.21.

[20]T. J. M. Zouros, D. H. Lee, and P. Richard, Phys. Rev. Lett. **62**, 2261 (1989).

[21]J. M. Cheshire, Proc. Phys. Soc. London **83**, 227 (1964).

[22]B. Crasemann, P. E. Koblas, T. C. Wang, H. E. Birdseye, and M. H. Chen, Phys. Rev. A **9**, 1143 (1974). We are grateful to J. H. Macek for drawing our attention to this paper.

[23]J. W. Cooper, Phys. Rev. A **9**, 2236 (1974).

[24]J. J. Bentley and R. F. Stewart, J. Comput. Phys. **11**, 127 (1973); J. Chem. Phys. **62**, 875 (1975).

[25]J. H. Hubbell, Wm. J. Veigle, E. A. Briggs, R. J. Brown, D. T. Cromer, and R. J. Howerton, J. Chem. Phys. Ref. Data **4**, 471 (1975), Eq. (32) [this has a typographical error; $|F(x,H_2)|$ should be squared] and Table IV, column 6.

[26]Ref. 25, Table IV, column 7.

[27]R. F. Stewart (private communication).

[28]J. S. Briggs and K. Taulbjerg, in *Structure and Collisions of Ions and Atoms,* edited by J. A. Sellin (Springer, Berlin, 1978), Sec. A.1.5.

[29]G. W. McClure, Phys. Rev. **166**, 22 (1968). As noted by McClure, the data also contain electron loss by capture, but this is a small effect.

[30]A. B. Wittkower, G. Levy, and H. B. Gilbody, Proc. Phys. Soc. London, Sect. B **91**, 306 (1967). The data points at 0.04 and 0.05 MeV/u have been omitted from Fig. 4, because they seem to be erroneous. See J. Hill, J. Geddes, and H. B. Gilbody, J. Phys. B **12**, 3341 (1979), and Ref. 29.

[31]M. B. Shah and H. B. Gilbody, J. Phys. B (to be published); M. B. Shah, T. V. Goffe, and H. B. Gilbody, *ibid.* **11**, L233 (1978).

[32]T. V. Goffe, M. B. Shah, and H. B. Gilbody, J. Phys. B **12**, 3763 (1979).

[33]P. M. Stier and C. F. Barnett, Phys. Rev. **103**, 896 (1956).

[34]C. F. Barnett and H. K. Reynolds, Phys. Rev. **109**, 355 (1958).

[35]L. I. Pivovar, V. M. Tubaev, and M. T. Novikov, Zh. Eksp. Teor. Fiz. **42**, 1490 (1962) [Sov. Phys.—JETP **14**, 20 (1962)].

[36]M. E. Rudd, T. V. Goffe, A. Itoh, and R. D. DuBois, Phys. Rev. A **32**, 829 (1985).

[37]M. Sataka, A. Yagishita, and Y. Nakai, J. Phys. B **23**, 1225 (1990).

[38]R. Anholt, X.-Y. Xu, Ch. Stoller, J. D. Molitoris, W. E. Meyerhof, B. S. Rude, and R. J. McDonald, Phys. Rev. A **37**, 1105 (1988).

[39]Yu Dong Wang and J. H. McGuire (unpublished).